Renewable Energy 185 (2022) 978–995

Contents lists available at ScienceDirect

Renewable Energy

journal homepage: www.elsevier.com/locate/renene

Load mitigation method for wind turbines during emergency shutdowns

Zhiyu Jiang [a, *], Yihan Xing [b]

[a] Department of Engineering Sciences, University of Agder, N-4898, Grimstad, Norway
[b] Department of Mechanical and Structural Engineering and Materials Science, University of Stavanger, Norway

ARTICLE INFO

Article history:
Received 30 March 2021
Received in revised form
6 October 2021
Accepted 14 December 2021
Available online 27 December 2021

Keywords:
Shutdown
Blade pitch control
Blade-root bending moment
Wind shear
Extreme load
Fatigue damage

ABSTRACT

Wind turbines experience countless shutdowns during their lifetimes. A shutdown is a transient process characterised by a pitch-to-feather manoeuvre of three blades. Such a pitch manoeuvre is often collective, open-loop, and can substantially slow the rotor speed within several seconds. However, undesirable structural responses may arise because of the imbalanced aerodynamic loads acting on the rotor. To address this issue, this paper proposes a method that actively adjusts the individual pitch rate of each blade during an emergency shutdown. This method is founded on a minimal intervention principle and uses the blade-root bending moment measurements as the only inputs. The control objective is to minimise the differences in the blade-root flapwise bending moment among the three blades during the shutdown. Using a high-fidelity aeroelastic model, we demonstrate the controller performance under representative steady wind conditions with vertical wind shear. Compared with the baseline shutdown strategy, the proposed method effectively reduces the maximum nontorque bending moment at the main shaft and the tower bottom bending moment; the reductions vary between 10% and 40% under the investigated conditions. The present work can be further extended to reduce structural fatigue damages or to handle complex loading scenarios of offshore wind turbines during shutdowns.

1. Introduction

Load control and mitigation has been an important theme for wind energy research since the inception of the wind industry. As wind turbines are subjected to dynamic loads due to the combined effects of external wind conditions and control actions, various mechanical (e.g., shafts and bearings) and structural components (e.g., blades and support structures) will encounter extreme loading [1,2] and fatigue damages [3,4] during their service lives. Today's wind turbines are designed with longer blades, higher tower, and greater tip speeds, and they become more flexible and susceptible to unwanted large vibrations. Accordingly, load control plays an increasingly critical role to alleviate undesirable structural loads and hence to avoid premature component failures.

For conventional wind turbines, there are primarily two categories of load mitigation methods. The first category achieves load reduction based on active blade pitch, whereas the second category requires additional damping devices (passive, semi-active or active) to be mounted on wind turbine structures. For the first category, an early work of Larsen et al. [5] suggested using local blade flow measurements in the individual blade pitch control and showed the effect of the proposed control strategy on the blade-root flapwise bending moment and tower-top moments. Still, this strategy involves installations of additional flow measurement devices on each blade, limiting its practical applications. Later Namik and Stol [6] applied individual pitch control to improve power output and reduce platform motions of floating wind turbines. For the second category, Zhang et al. [7,8] demonstrated the promising potential of damping devices for mitigating the blade and tower vibrations. Nevertheless, these devices require additional installation and maintenance costs. These applications are also limited to normal power production of wind turbines with cyclic loading behaviour.

Different from the normal operational conditions, shutdowns are transient stages during which a wind turbine is switched to a stand-by state [9]). Fig. 1 illustrates the normalised power time series of a wind farm during one month in 2007. As shown, the power dropped to zero intermittently, indicating the occurrences of shutdowns of individual wind turbines in the wind farm.

* Corresponding author.
E-mail address: zhiyu.jiang@uia.no (Z. Jiang).

https://doi.org/10.1016/j.renene.2021.12.068

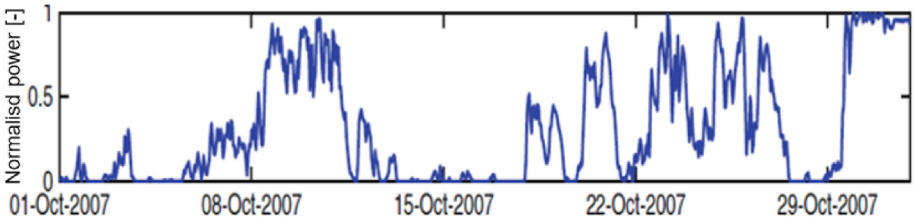

Fig. 1. Illustration of normalised power time series of a 20-MW wind farm, adapted and reproduced from Ref. [10].

There exist various causes for shutdowns and these include unsuitable wind conditions, human intervention, and faults of critical components [11]. For pitch-regulated wind turbines, a shutdown normally involves collectively pitching the three blades to feather, but the strategy may vary depending on wind turbine specifications [12]. As a shutdown may induce excessive structural responses, pertinent design load cases are specified by international design standards. For example, IEC 61400-1 [13] dictates that fatigue analysis must be considered for normal shutdown and ultimate strength analysis must be considered for emergency shutdown. However, the load cases related to normal and emergency shutdowns are not well-documented in literature, and only a few attempts have been made to study the transient loads occurring during the shutdown events.

Jiang et al. [14] examined the effect of different collective pitch rates and grid conditions on the dynamic responses of wind turbines. Compared with the one-stage procedure with a fixed pitch rate, the two-stage pitching procedure with reduced pitch rate at the second stage has no impact on the extreme responses which occur shortly after the initiation of shutdown. Following this work Nejad et al. [15] studied the impact of emergency shutdown on the drivetrain responses and found that the rotor imbalance during a shutdown can induce detrimental nontorque loading on the main bearings. In two separate works Louzael et al. [16] and Luan et al. [17] both investigated the responses of semi-submersible floating wind turbines during similar shutdown conditions and reported large stress cycles in the structural members during the collective pitching procedure.

The above-mentioned works consider turbulent wind conditions during shutdowns. As the dynamic responses of wind turbines depend on blade azimuth and instantaneous wind field upon shutdown, a few numerical simulations with random seed numbers are needed to capture the variability of responses. Besides wind turbulence, the wind speed profile is another source of spatial variation of wind speed and affects the dynamic loads as well as power production of wind farms [18]. In most literature about the effect of wind shear, the wind speed shear has been widely described by the following power law profile:

$$V(z) = V_0 \left(\frac{z}{z_0}\right)^{\alpha} \tag{1.1}$$

where z_0 is a reference height and V_0 is the wind speed at this height. V is the horizontal wind speed at height z. α is the shear exponent. For a given shear exponent, the wind speed increases monotonically with the height; see Fig. 2 (left). Higher values of the shear exponent lead to greater variation of the wind speed across the height based on Eq. (1.1); see Fig. 2 (right).

Although the wind shear exponent is generally taken as 0.14 or 0.2 [13], the wind shear exponent is not constant and depends on atmospheric conditions, temperature, seasons of the year, and nature of terrain. For instance Ref. [18], reported that the average exponent can vary between 0.11 and 0.36 among different regions. Another report [19] found that 7.3% of wind shear coefficients were distributed between 0 and 0.14, and 91.9% of them were above 0.14; while a 0.8% of wind shear coefficients were negative. In this study, two representative wind shear exponents of 0.14 and 0.7 are considered for land-based wind turbines with normal and large wind shears, respectively.

We are motivated by the need to mitigate the structural loads during shutdowns under wind shear conditions. Inspired by the individual pitch control method for operational wind turbines, we propose a control method that actively adjust the individual blade pitch during the shutdown process in this work. We focus on the emergency shutdown with a high pitch rate and consider steady wind conditions with shear flow. These conditions facilitate the understanding of the transient process and are also representative of scenarios with rotor imbalance. This article contributes to improved shutdown strategies for existing bottom-fixed wind turbines instrumented with blade-root sensors like strain gauges [20]. The proposed method using a feedback-controlled shutdown, hereafter the FCS method, can be further developed and adapted to commercial wind turbines for load mitigation purposes. In the following, Section 2 describes the fundamental physics of pitch-to-feather shutdown and the main idea of the adjusted pitch rate, Section 3 presents the controller design and the numerical simulation in FAST-SIMULINK [21], Section 4 shows the controller tuning results of the NREL 5-MW wind turbine, Section 5 discusses the numerical simulation results and highlights the effect of the FCS method, Section 6 draws the conclusion.

2. Shutdown scenario of pitch-regulated wind turbines

2.1. Physics of the emergency shutdown

For pitch-regulated wind turbines, aerodynamic braking by pitching the blade (rather than mechanical braking) is the primary measure for shutdown. Fig. 3 and Fig. 4 show representative time histories of the rotor speed and the collective blade pitch angle, respectively. As shown, the rotor revolution speed experiences a significant reduction shortly after the shutdown is initiated. According to the conventional open-loop strategy, i.e., without any feedback control, the pitch angles of all three blades are increased monotonically and collectively to a feathered position at a fixed pitch rate. A hydraulic pitch system should be designed with a fail-safe shutdown mechanism. If there is no backup power supply for the pitch system during an emergency shutdown, the pitch rate will depend on the accumulator capacity [22]. However, if there is an uninterruptible power supply, the pitch rate can be adjusted in a controlled manner, which is relevant for the present work.

During this process, the aerodynamic forces on the blade experience drastic changes, and Fig. 5 schematises the main force components at two selected time instants. In the figure, the rotor is rotating in the clockwise direction and the free stream wind, V_0, is propagating into the paper and perpendicular to the rotor plane. At Time instant 1, the shutdown has just been initiated, and the

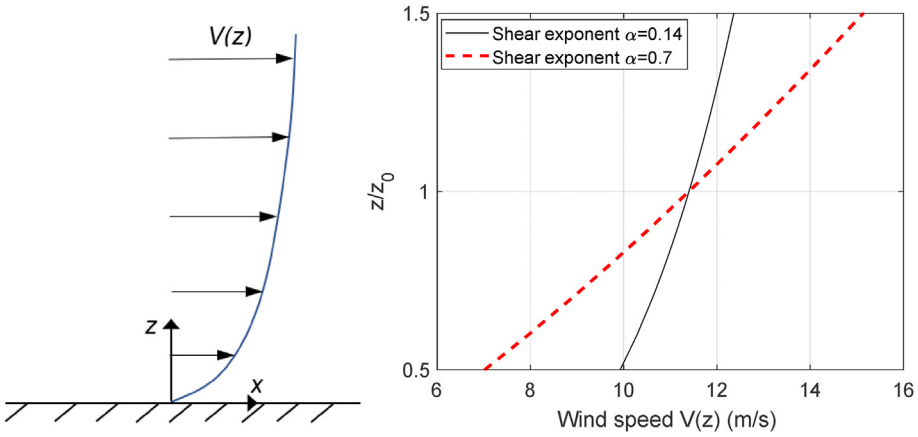

Fig. 2. Illustration of a vertical wind shear (left) and two wind profiles (right).

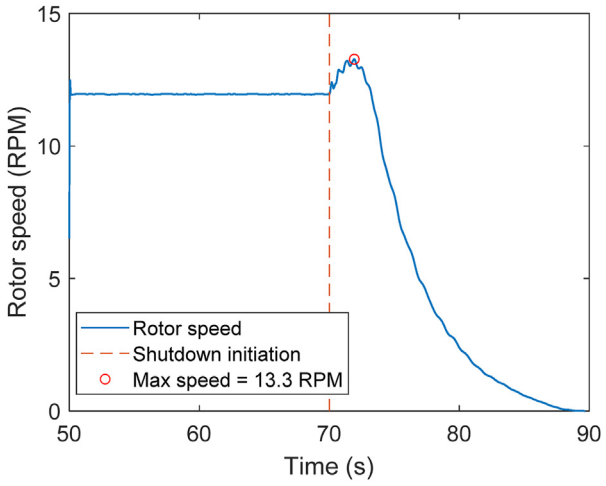

Fig. 3. Time history of rotor speed during a shutdown.

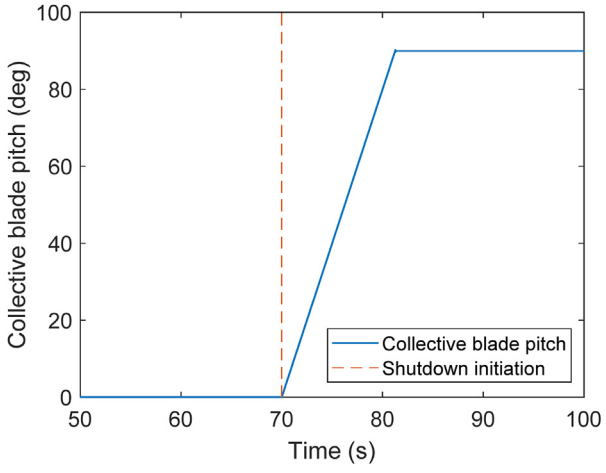

Fig. 4. Time history of collective blade pitch during a shutdown.

aerodynamic forces are similar to those of an operating wind turbine. The sketched blade section has a small pitch angle for above-rated wind speed and the operating angle of attack (α_1) is positive and typically below 20 deg so that stall does not occur. $V_{rel,1}$ is the relative wind speed seen by the airfoil. At this moment, the components of the lift (L_1) and drag (D_1) in the rotor plane points towards the left, delivering a positive aerodynamic torque. Time instant 2 is another time shortly after instant 1, e.g., 1–2 s. Because of the fast pitching of the blades, the angle of attack flips its direction to the other side of the chord and is negative. This is denoted α_2. Consequently, the lift (L_2) flips its direction, and the total sum of the lift and drag creates a reversed aerodynamic torque which stops the rotor.

2.2. Blade response during shutdown

Understanding the blade responses during an emergency shutdown is key to the problem herein. Fig. 6 shows the construct of a rotating blade upon the initiation of shutdown.

As seen, the blade can be rotated in pitch about the pitch axis which extends spanwise, perpendicular to the blade root flange. The blade pitch is often defined as zero when the chord of the airfoil close to the tip lies in the rotor plane [23]. Bending of the blades is defined in flapwise and edgewise (lead-lag) directions, which at zero pitch correspond to out of and in rotor plane directions. The blades may also deform in torsion (twist), whereby the airfoil cross sections are rotated. The blade-root strain gauges are usually available which can give information of the bending moment in edgewise and flapwise direction [24]. During operation, the flapwise bending moment can be characterised by a stochastic Gaussian process as this moment is directly affected by the turbulent wind loads, while the edgewise bending moment has a significant sinusoidal term owing to the effects of gravity [2].

During emergency shutdowns, the extreme structural responses (e.g., shaft nontorque bending moment and tower-bottom bending moment) only occur during the first few seconds when the flapwise bending moment is still more sensitive to the wind loads than to the edgewise bending moment. Time histories of these blade root bending moments during shutdown are presented in Fig. 7 and Fig. 8. As shown, the flapwise bending moment remains positive during operation. After the shutdown is initiated at 70 s, it experiences a sudden change in the direction from positive to negative values due to the pitching action and the effect on the aerodynamic angle of attack (see Fig. 5). In contrast, the edgewise bending moment experiences cyclic oscillations during operation and shutdown. Because of the rotor speed reduction, the maximum edgewise bending moment during shutdown is not larger than that during operation. In this work, the difference in the flapwise bending moment among the three blades are hypothesised to be an important variable to reduce. This is because the emergency shutdown is a very short process and the loading characteristics of

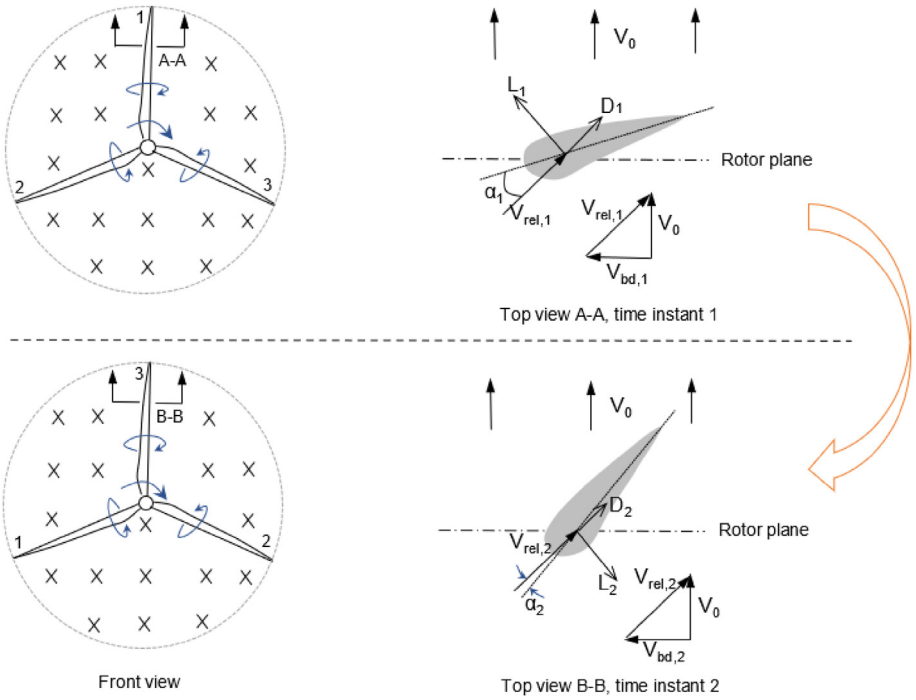

Fig. 5. Schematic of aerodynamic forces acting on a blade cross section during shutdowns.

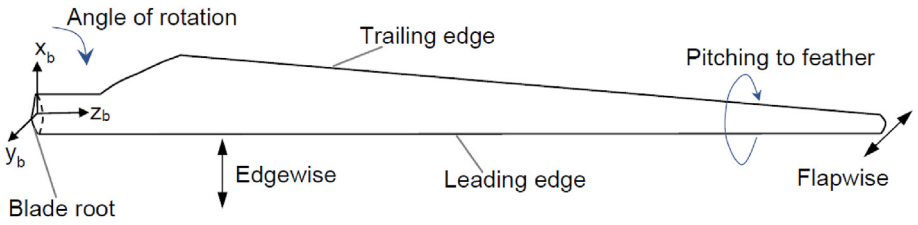

Fig. 6. Schematic of a wind turbine blade during pitch-to-feather shutdown.

the flapwise bending during the first rotor revolution will be like that of a blade during operation [2].

Fig. 9 demonstrated a spatial variation of the horizontal wind speed under a normal wind shear calculated by Eq. (1.1). Although the NREL 5-MW wind turbine [25] has a blade length of 63 m which can be 40% shorter than the longest commercial blade in existence today, there is still a velocity difference of approximately 2 m/s between the neighbouring blade tips because of the normal wind shear. The velocity difference across the rotor plane causes

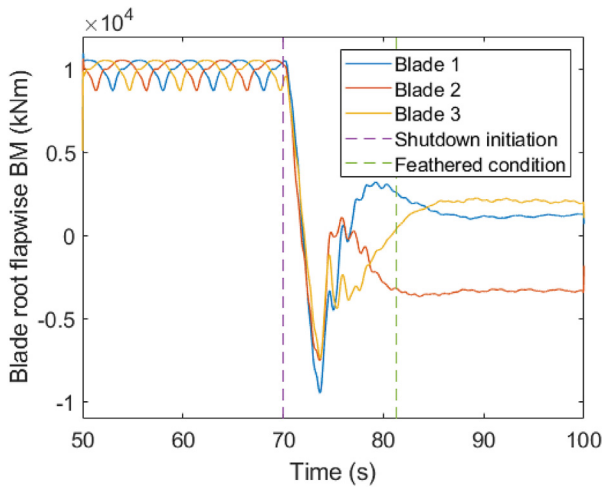

Fig. 7. Time history of flapwise bending moment of blades during a shutdown.

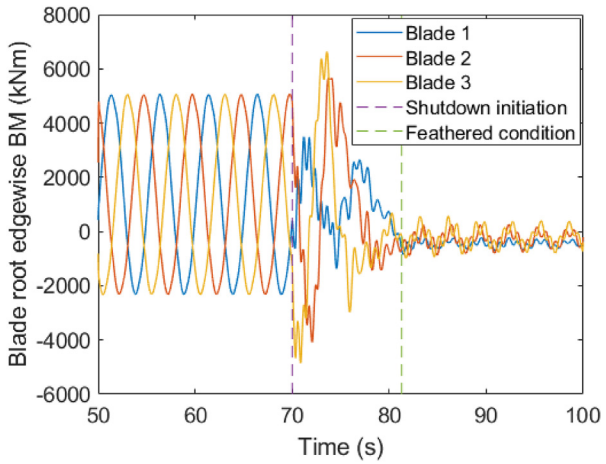

Fig. 8. Time history of edgewise bending moment of Blade 1 during a shutdown.

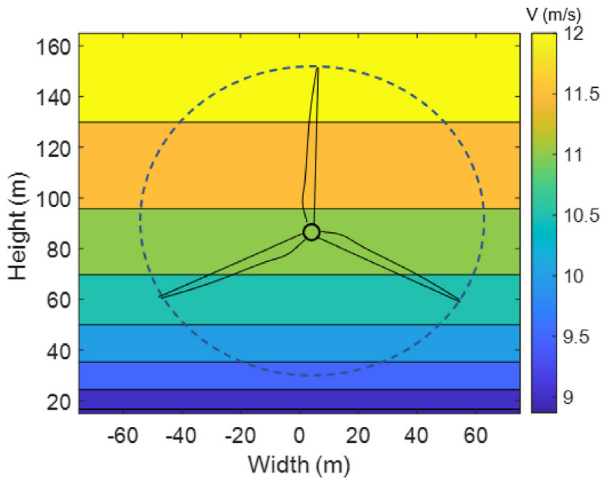

Fig. 9. Illustration of a 5-MW wind turbine rotor in shear flow with the hub-height velocity V_{hub} = 11.4 m/s and a shear exponent of 0.14.

unevenly distributed aerodynamic loads on the blades during shutdowns. This rotor imbalance will further affect the shaft non-torque bending moment and other structural responses.

3. Numerical simulation

In this section, the controller design philosophy behind the FCS method is first presented. Then, the numerical framework for carrying the current time-domain simulations is described in detail.

3.1. Control philosophy

As described in Section 2.2, the flapwise bending moment is more important than the edgewise bending moment during shutdown and contributes more significantly to the extreme loads. Hence, the objective of the controller is to minimise the differences in the blade root flapwise bending moments between the three blades during the shutdown events, because these moments are measurable and controllable for most commercial wind turbines with blade-root strain gauges and blade pitch systems. This difference in the flapwise bending moment is denoted as an error term expressed by Eq. (3.1):

$$M_{y,i,err} = |M_{y,i}| - M_{y,ave} \tag{3.1}$$

where $M_{y,i}$ is the flapwise bending moment for blade no. i ($i = 1,2,3$) and $M_{y,ave}$ is the average flapwise bending moment calculated as:

$$M_{y,ave} = \frac{\sum_1^3 |M_{y,i}|}{3} \tag{3.2}$$

We design a proportional-integral-derivative (PID) controller because of its simplicity for feedback control of the individual blade pitch. At each time instant t_s after the initiation of shutdown, the commanded blade pitch rate for each pitch actuator is given by Eq. (3.3):

$$\dot{\theta}_{i,com} = k_P \cdot M_{y,i,err} + k_I \cdot \int_0^{t_s} \cdot M_{y,i,err} dt + k_D \cdot \frac{dM_{y,i,err}}{dt} \tag{3.3}$$

where k_P, k_I, and k_D are respectively the proportional, integral, and derivative coefficients of the PID controller. Note that the commanded blade pitch rates are saturated to the maximum and minimum allowable rates based on the pitch motor capacity. The model implementation for the controller design is done in the Pitch Controller Block as illustrated in Fig. 13.

3.2. Wind turbine model

The NREL 5-MW reference wind turbine [25] is considered in this work. This is an academic pitch-regulated wind turbine model widely used by the wind energy community. For the aeroelastic simulations in FAST, an operational controller (DISCON) is available which includes collective blade pitch and generator torque control. Validation campaigns of FAST against other numerical codes have been extensively carried out before; see Refs. [26,27]. The wind turbine shutdown strategies, including the open-loop collective pitch-to-feather and the FCS method (Eq. (3.1) - (3.3)) are implemented through SIMULINK.

3.3. Simulation procedure

As illustrated in Fig. 10, each aeroelastic simulation in FAST under a given wind condition can be divided into two stages. In stage 1, the wind turbine has normal power production using the baseline controller (DISCON) [25]; this is referred to as the open loop (OL) method in the rest of the paper. This controller allows collective pitch control and generator torque control during stage 1 and rotor speed and blade pitch angle are used for the feedback control. When the wind turbine switches to the shutdown mode in stage 2, SIMULINK is used to activate the pitch controller (Ref. Section 3.4.1). Only the blade pitch references and blade root flapwise bending moments are used in the feedback. To highlight the effect of the active pitch-to-feather method, no mechanical brake or grid connection is considered in all simulations. As shown by Jiang et al. [14], the influence of mechanical brake is relatively small compared with that of the aerodynamic brake.

3.4. Simulation platform

The simulation is implemented using the FAST version 8 with SIMULINK. The simulation architecture is illustrated in Fig. 11 and consists of the following main blocks:

- Nonlinear wind turbine block: This block implements the Matlab S-function that runs the FAST program which computes the aeroelastic responses of the wind turbine structures in the time domain.
- Pitch controller: This block sends the pitch actuator angle commands for all three blades to the FAST Nonlinear Wind Turbine block. This block is modified and presented in Fig. 12.
- Generator controller: This block sends the generator torque and power commands to the Nonlinear Wind Turbine block. This block is modified and presented in Fig. 13. Each simulation contains two stages, the normal operation and the shutdown. During the normal operation ($t < t_s$), the generator-torque controller computes the generator torque as a function of the filtered generator speed [21]. Upon shutdown ($t > t_s$), the generator is disconnected, and the generator torque becomes zero. Disconnecting the generator torque upon shutdown is a conservative approach for the loads analysis; see Jiang et al. [14].
- Yaw controller: This block sends the yaw actuator command to the Nonlinear Wind Turbine block. This block is not used in the present work.
- High-speed shaft brake: This block sends the high-speed shaft brake command to the Nonlinear Wind Turbine block. This block is not used in the present work.

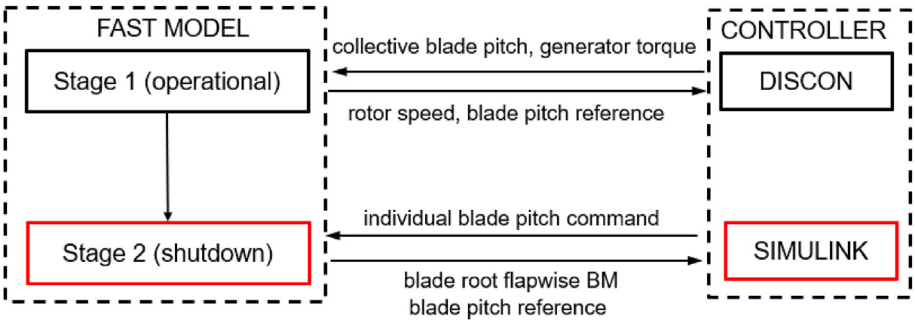

Fig. 10. Simulation procedure.

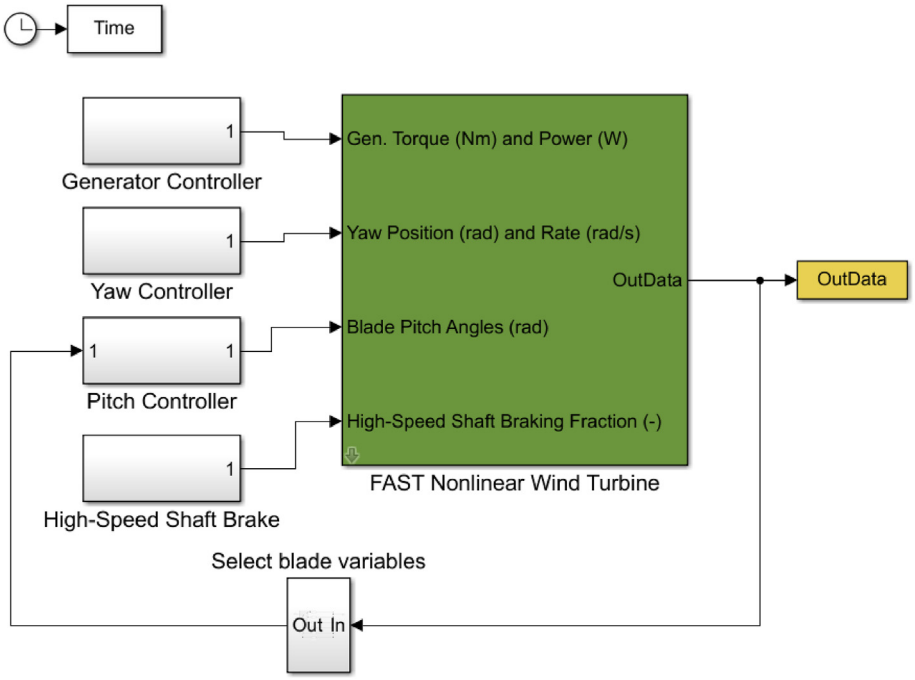

Fig. 11. FAST-SIMULINK model.

3.4.1. Blade pitch controller

The SIMULINK pitch controller block is presented in Fig. 12. This block activates the shutdown sequence when a shutdown event is defined. This means the commanded blade pitch angles are calculated based on the controller design defined in Section 3.1 if shutdown is activated, otherwise the commanded blade pitch angles will be that of the time series from the FAST/DISCON model. The block consists of the following four blocks:

- Inputs: This block transfers the desired nominal blade pitch rate and the precalculated time series of the blade pitch angles when no shut down event is simulated.
- Low pass filter: This block filters out the high frequency responses from the calculations to ensure a robust simulation process. A cut-off frequency of 10 Hz is used [25].
- Error calculation: This block implements the blade root flapwise bending moments error calculation as presented in Eq. (3.1) and Eq. (3.2), respectively.
- Pitch command: This block implements the pitch command models which calculates the commanded pitch based on the blade root flap wise bending moments errors obtained. The control methodology is based on the PID control as presented in Eq. (3.3).

To facilitate understanding, a schematic of the implemented feedback loop during a shutdown is illustrated in Fig. 14. The communication between the wind turbine block and the controller block (dashed line) occurs every 0.00625 s during the time-domain simulation [21]. Note that the open-loop shutdown strategy [14] is also implemented in SIMULINK. This strategy does not require any feedback and is not shown here.

4. Controller tuning

The purpose of controller tuning is to find the optimal PID coefficients (k_P, k_I, and k_D) such that the FCS method achieves desired load mitigation effects.

4.1. Tuning procedure

The controller tuning procedure is illustrated in Fig. 15. The first step involves selection of load cases. Here, we consider three hub-

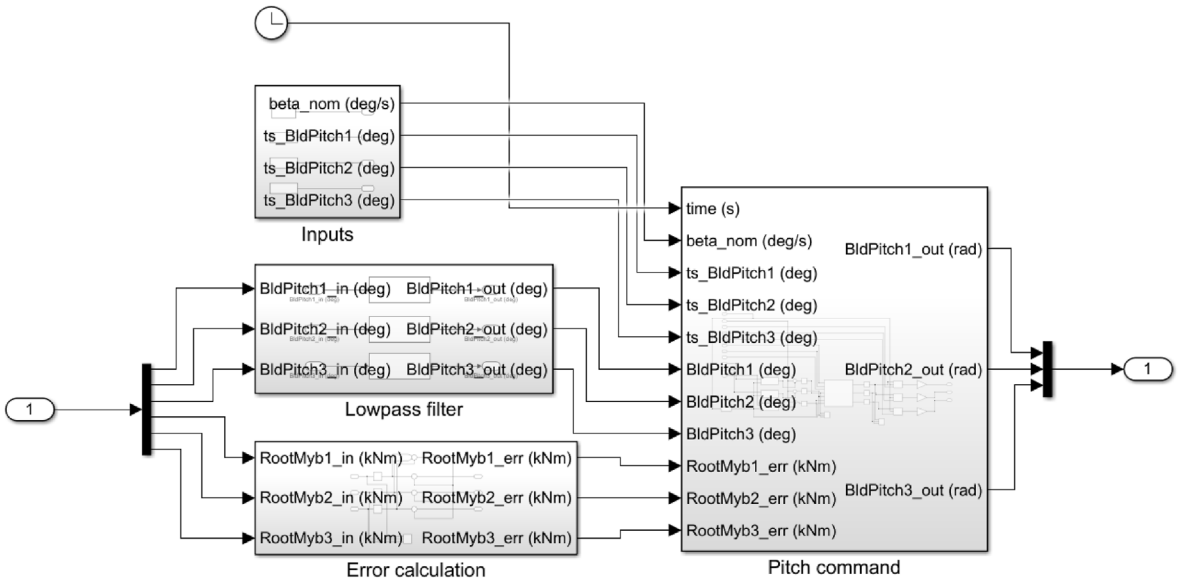

Fig. 12. SIMULINK pitch controller block.

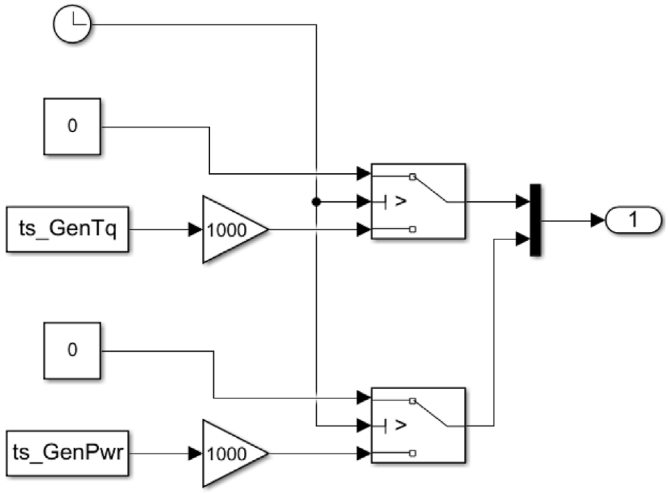

Fig. 13. SIMULINK generator controller block.

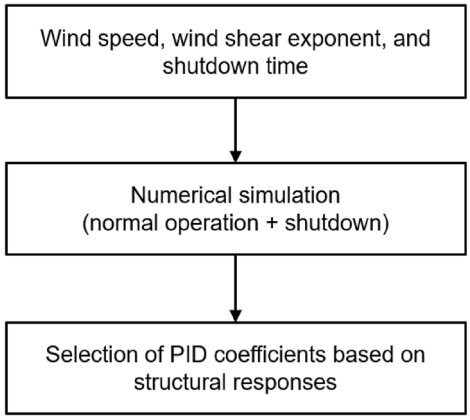

Fig. 15. Flowchart for controller tuning.

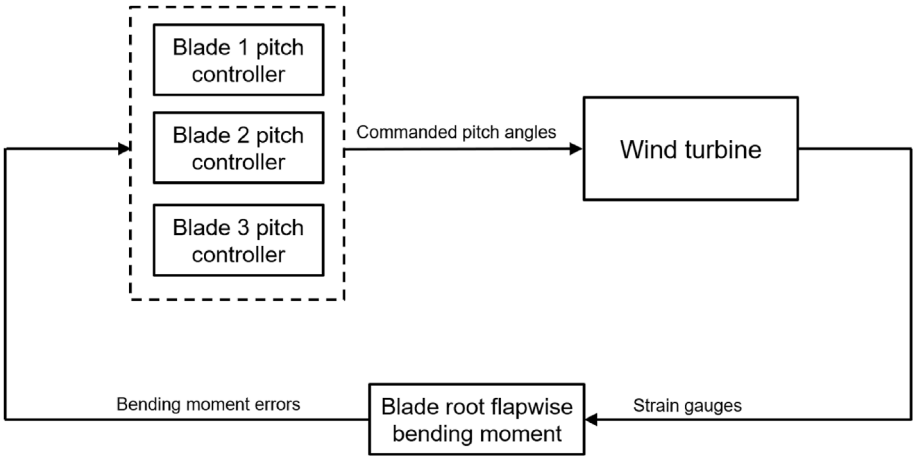

Fig. 14. Blade pitch controller feedback loop during shutdowns.

Table 1
Load cases considered in the study.

Parameter	Symbol	Numbers studied	Units
Wind velocity	V	8, 11.4, 18	m/s
Shear exponent	A	0.14, 0.7	–
Shutdown time	t_s	70, 71, 72, 73, 74, 75	s
Proportional coefficient	k_P	0, 5e-7, 2.5e-6, 1.25e-5, 6,25e-5, 0.00313	deg/(s·kNm)
Integral coefficient	k_I	0, 5e-7, 2.5e-6, 1.25e-5, 6,25e-5, 0.00313	deg/(s^2·kNm)
Derivative coefficient	k_D	0, 5e-7, 2.5e-6, 1.25e-5, 6,25e-5, 0.00313	deg/kNm

Table 2
List of control coefficients, extreme wind shear.

V (m/s)	t_s (s)	Azimuth (deg)	Most optimal control coefficients*		
			k_P	k_I	k_D
8	70	46	6.25E-04	3.13E-04	1.25E-05
	71	104	1.25E-04	1.25E-04	3.13E-04
	72	163	3.13E-03	3.13E-03	3.13E-04
	73	221	6.25E-04	6.25E-04	3.13E-04
	74	273	6.25E-04	6.25E-04	1.25E-05
	75	316	2.50E-05	2.50E-05	3.13E-04
	Coeff. set B		8.58E-04	8.06E-04	2.13E-04
11.4	70	39	2.50E-05	3.13E-04	3.13E-04
	71	115	6.25E-04	3.13E-04	3.13E-04
	72	194	6.25E-04	2.50E-06	6.25E-05
	73	272	1.25E-04	6.25E-05	1.25E-05
	74	341	2.50E-05	3.13E-04	6.25E-05
	75	36	1.25E-04	2.50E-06	3.13E-04
	Coeff. set B		2.58E-04	1.68E-04	1.79E-04
18	70	111	1.25E-04	6.25E-05	6.25E-05
	71	186	6.25E-04	1.25E-05	3.13E-04
	72	259	6.25E-04	3.13E-04	3.13E-04
	73	319	6.25E-04	6.25E-05	3.13E-04
	74	7	1.25E-04	3.13E-04	6.25E-05
	75	43	5.00E-06	2.50E-06	3.13E-04
	Coeff. set B		3.55E-04	1.28E-04	2.29E-04
Coeff. set C			4.91E-04	3.67E-04	2.07E-04

*Coeff. set A is marked in red; Coeff. set B in blue, Coeff. set C in black.

Table 3
List of control coefficients, normal wind shear.

V (m/s)	t_s (s)	Azimuth (deg)	Most optimal control coefficients*		
			k_P	k_I	k_D
8	70	318	3.13E-03	1.25E-05	1.25E-05
	71	14	3.13E-03	3.13E-03	3.13E-04
	72	72	3.13E-03	3.13E-03	1.25E-05
	73	128	5.00E-06	5.00E-06	6.25E-05
	74	179	3.13E-03	3.13E-03	3.13E-04
	75	222	3.13E-03	3.13E-03	3.13E-04
	Coeff. set B		2.61E-03	2.09E-03	1.71E-04
11.4	70	342	3.13E-03	5.00E-07	6.25E-05
	71	57	6.25E-04	6.25E-05	3.13E-04
	72	136	3.13E-03	2.50E-06	6.25E-05
	73	213	3.13E-03	2.50E-06	3.13E-04
	74	280	6.25E-04	3.13E-04	3.13E-04
	75	334	3.13E-03	2.50E-06	3.13E-04
	Coeff. set B		2.29E-03	6.38E-05	2.29E-04
18	70	105	2.50E-05	2.50E-06	3.13E-04
	71	180	3.13E-03	6.25E-05	3.13E-04
	72	252	3.13E-03	5.00E-07	3.13E-04
	73	314	6.25E-04	3.13E-04	1.25E-05
	74	2	3.13E-03	3.13E-04	3.13E-04
	75	39	5.00E-06	3.13E-04	3.13E-04
	Coeff. set B		1.67E-03	1.67E-04	2.63E-04
Coeff. set C			2.19E-03	7.72E-04	2.21E-04

*Coeff. set A is marked in red; Coeff. set B in blue, Coeff. set C in black.

height wind speeds ($V = 8$, *11.4* and 18 m/s), two wind shear exponents (α=*0.14, 0.7*) and six shutdown times ($t_s = 70, 71, \ldots, 75$ *s*) in our numerical simulations. The three wind speeds (below-rated, rated, and above-rated) represent different operational regions of the wind turbine prior to shutdowns. For the rated wind speed, the difference in the blade azimuth angle is approximately *60 deg* between two neighbouring shutdown times, e.g., $t_s = 70$ *and 71 s*. The two wind shear exponents are used for the normal wind shear and extreme wind shear conditions, respectively, and the latter is expected to cause larger rotor imbalance during shutdown.

The second step involves numerical simulations using the simulation platform described in Section 3.4 for the selected load cases. For each wind speed and wind shear condition, six shutdown cases with shutdown times 1 s apart are considered to capture the variations in the blade azimuth upon shutdown. As shown in Table 1, A range of k_P, k_I, and k_D coefficients are chosen for the simulations based on knowledge of wind turbine pitch controllers, although these ranges only form a subset of the total design space. The total simulation time in FAST under each steady wind condition is 10 min [13], of which approximately 100 s are useful because of

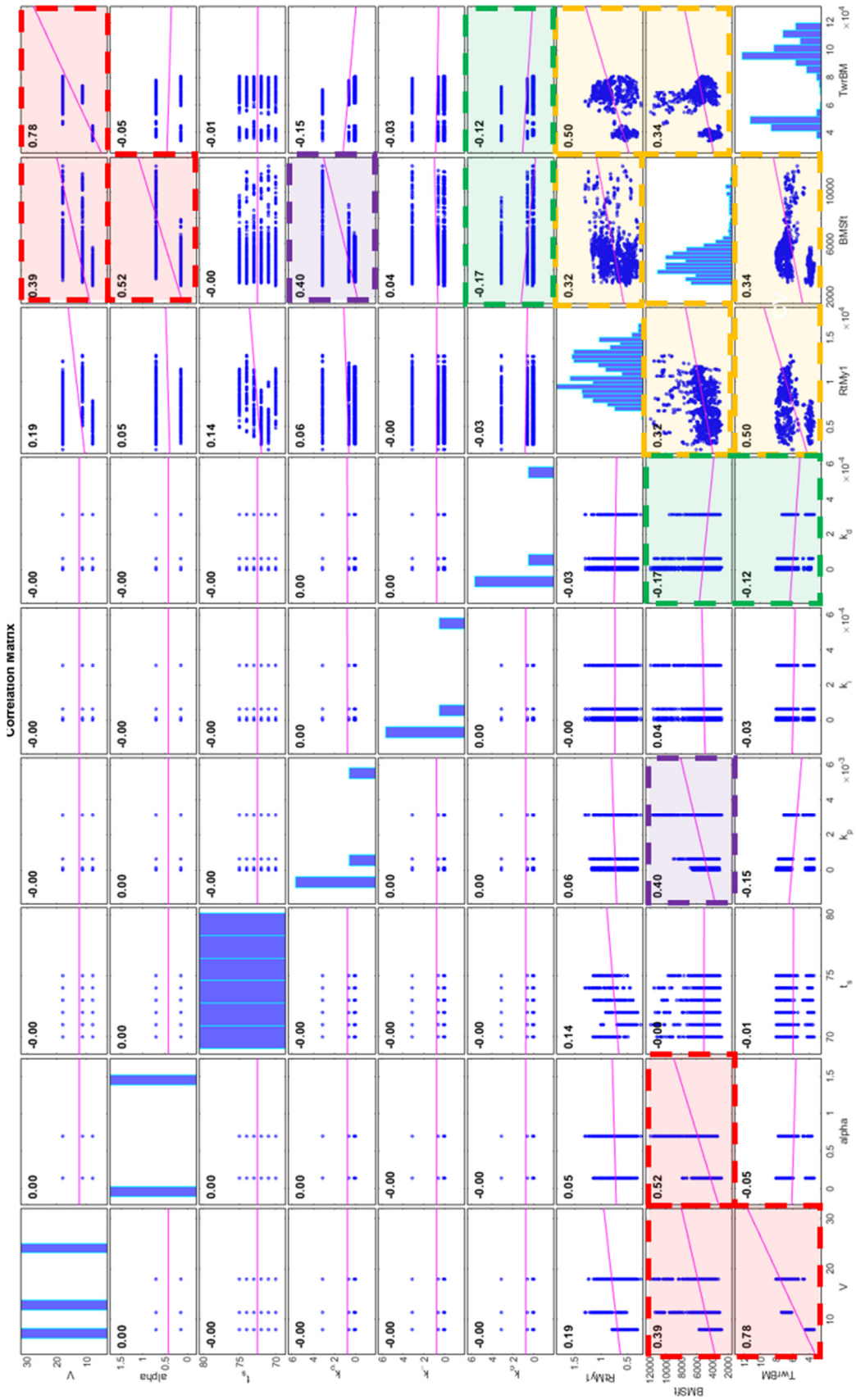

Fig. 16. Parametric correlation matrix.

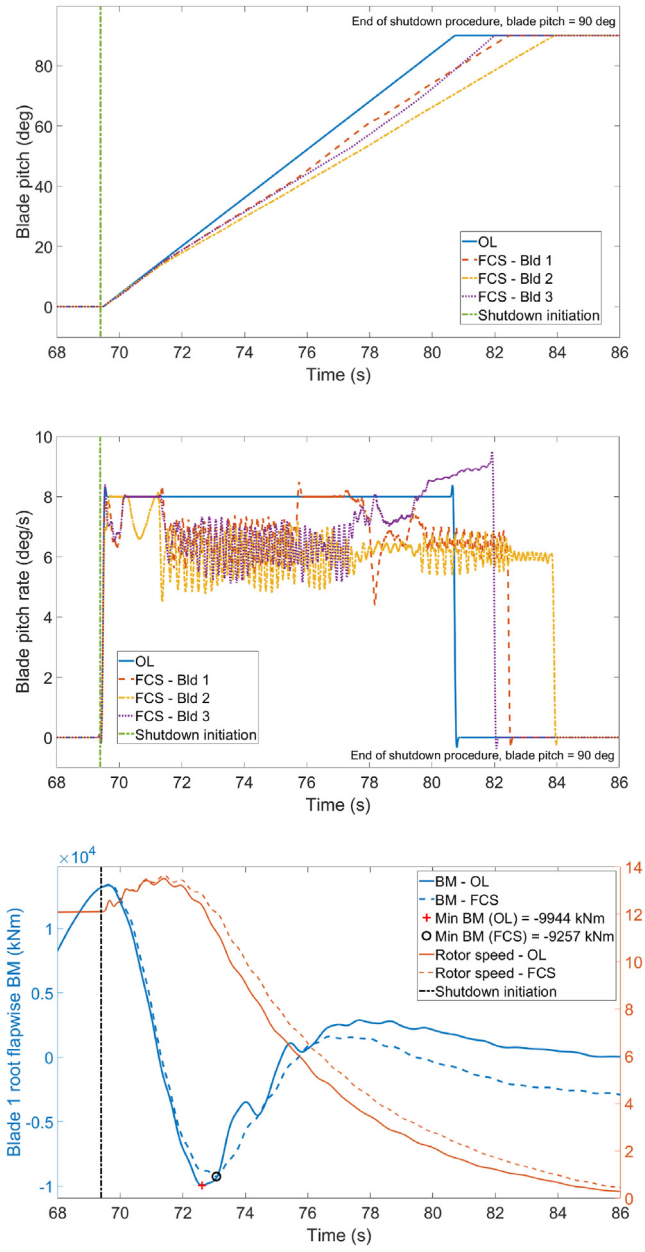

Fig. 17. A. Time series of blade pitch, $V = 11.4$ m/s at hub height, extreme wind shear, shutdown at azimuth = 0 deg, Coefficients set C.
Fig. 17B. Time series of blade pitch rate, $V = 11.4$ m/s at hub height, extreme wind shear, shutdown at azimuth = 0 deg, Coefficients set C..
Fig. 17C. Time series of blade 1 root flapwise BM and rotor speed, $V = 11.4$ m/s at hub height, extreme wind shear, shutdown at azimuth = 0 deg, Coefficients set C.

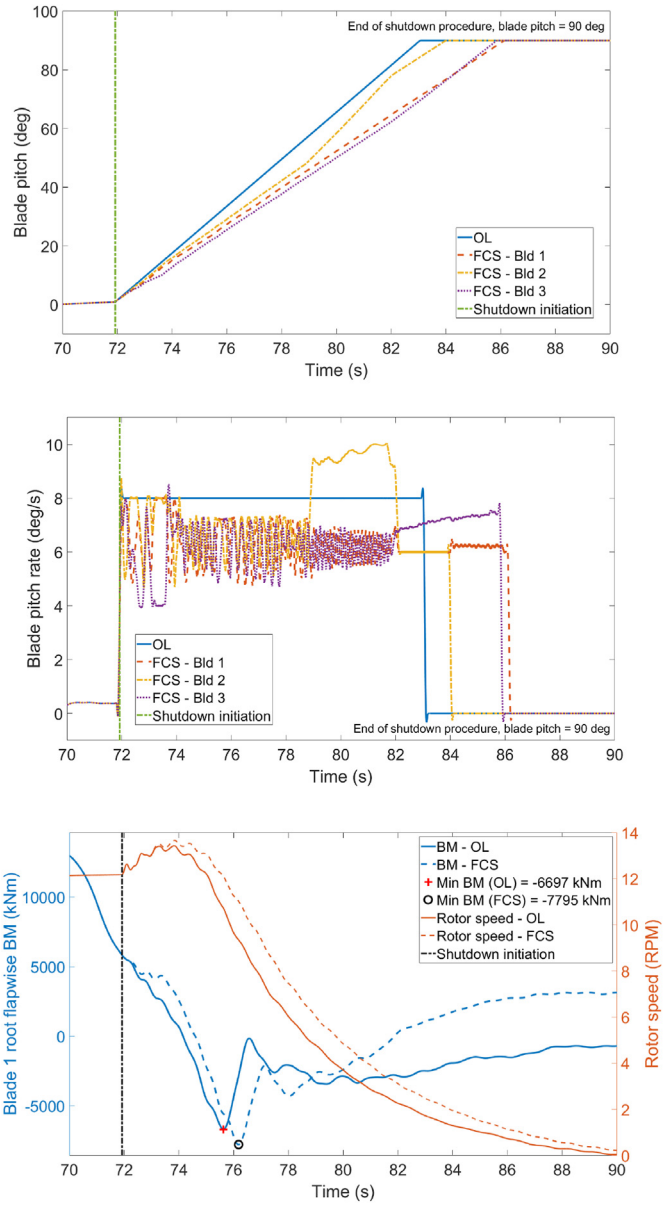

Fig. 18. A. Time series of blade pitch, $V = 11.4$ m/s at hub height, extreme wind shear, shutdown at azimuth = 180 deg, Coefficients set C.
Fig. 18B. Time series of blade pitch rate, $V = 11.4$ m/s at hub height, extreme wind shear, shutdown at azimuth = 180 deg, Coefficients set C.
Fig. 18C. Time series of blade 1 root flapwise BM, $V = 11.4$ m/s at hub height, extreme wind shear, shutdown at azimuth = 180 deg, Coefficients set C.

the quick decay of the responses. In total, 7776 simulations are carried out based on an orthogonal design of experiments.

In the final step, the PID coefficients are selected. As the shutdown conditions are transient load cases, several structural responses of a wind turbine experience large vibrations during the shutdown procedure. In this work, the main shaft equivalent bending moment ($M_{shaft,eq} = \sqrt{M_{shaft,y}^2 + M_{shaft,z}^2}$) is used as the sole indicator when selecting the coefficients. This moment is representative of the nontorque bending loads acting on the main bearing. As a resultant of the uneven blade-root bending moments, the nontorque bending moments are detrimental to the fatigue lifetimes of drivetrain components [4,28]. For each wind shear and each wind speed of 8, 11.4 and 18 m/s, six sets of most optimal control coefficients (Coefficients set A) are found: one set for each shutdown time or azimuth. These six sets of coefficients are then averaged to obtain the averaged coefficients for each wind speed (Coefficients set B). The Coefficients set B for each wind speeds are then further averaged to give the final wind speed-averaged coefficients (Coefficients set C). This procedure is a simplified way to average the influence of different shutdown conditions, e.g., azimuth or shutdown time, and condition-specific weights or gain scheduling can be applied to further optimise the controller performance. Using the procedure laid out in Fig. 15, the control coefficients for extreme wind shear and normal wind shear are presented in Table 2 and Table 3, respectively. It can be observed that the most suitable controller coefficients vary from case to case and the k_P and k_D values are often substantially larger than the k_I

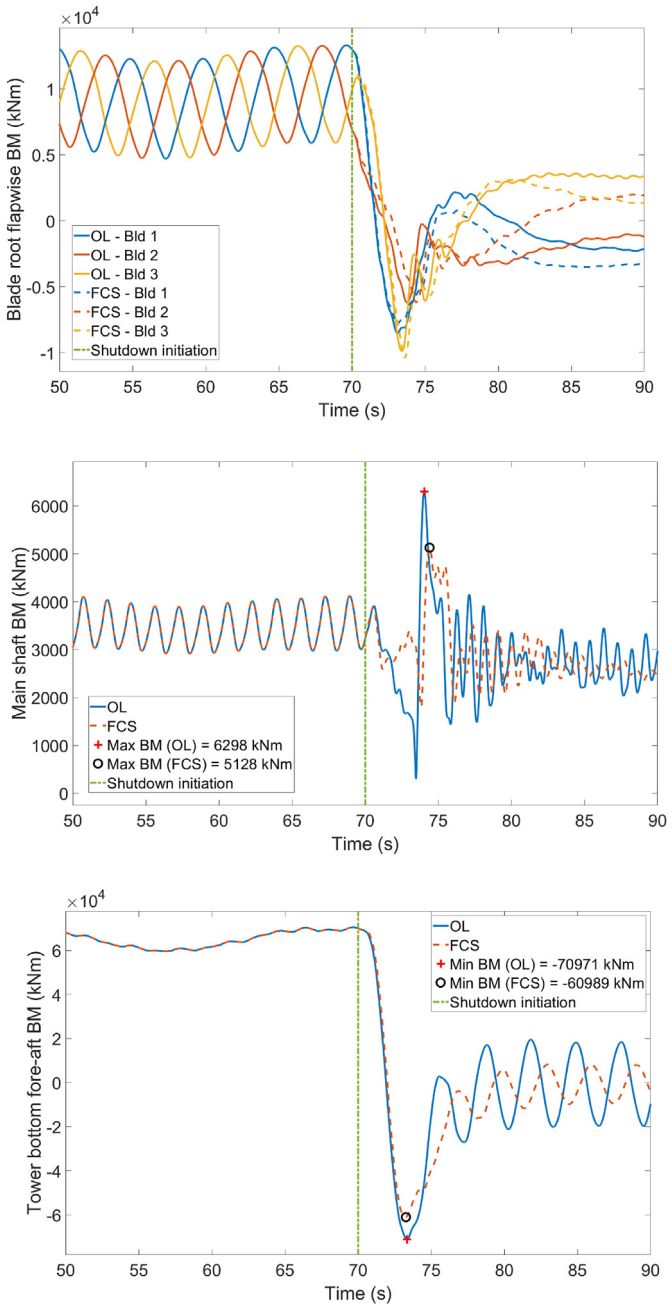

Fig. 19. A. Time series of blade root flapwise BM, $V = 11.4$ m/s at hub height, extreme wind shear, Coefficients set C.
Fig. 19B. Time series of main shaft BM, $V = 11.4$ m/s at hub height, extreme wind shear, Coefficients set C.
Fig. 19C. Time series of tower base fore-aft BM, $V = 11.4$ m/s at hub height, extreme wind shear, Coefficients set C.

values. This indicates that the error derivatives of the flapwise bending moments are important, and the design of a proper PID controller for the transient scenarios can be more challenging than that for the operational scenario where the optimum PID coefficients of the blade pitch controller can be analytically derived [25]. Although Coefficients set A can be regarded as the recommended PID coefficients here for load mitigation purposes, numerical simulation results from Coefficients sets A and C will be presented in Section 5 to highlight the influence of these coefficients on dynamic responses.

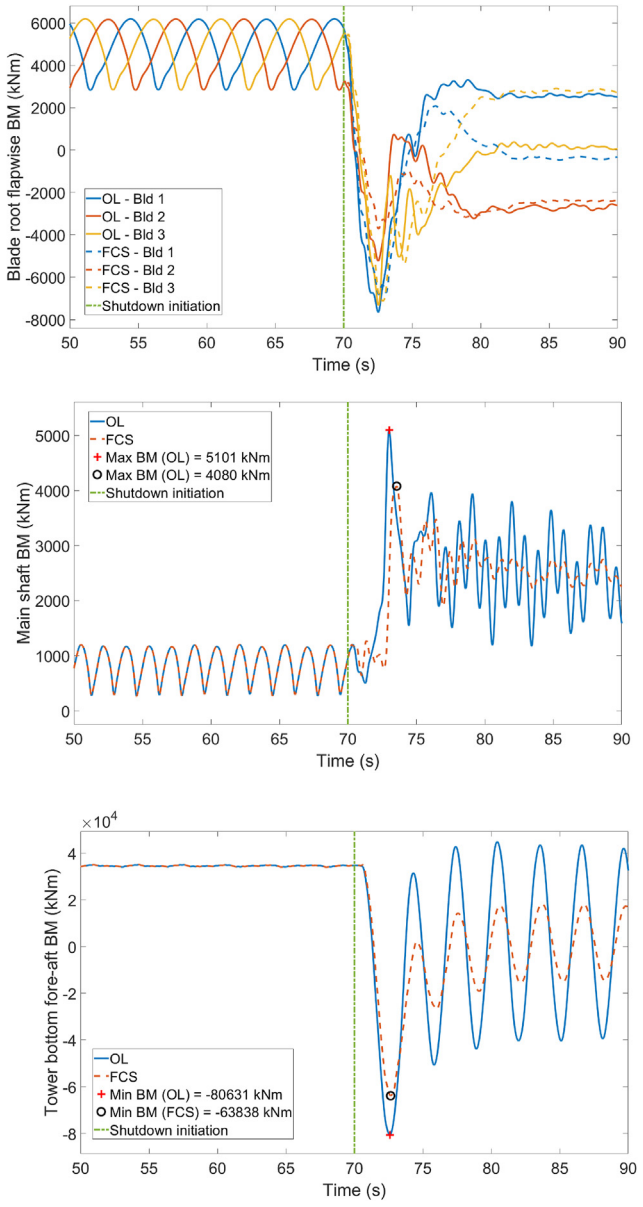

Fig. 20. A. Time series of blade root flapwise BM, $V = 18$ m/s at hub height, normal wind shear, Coefficients set C.
Fig. 20B. Time series of main shaft BM, $V = 18$ m/s at hub height, normal wind shear, Coefficients set C.
Fig. 20C. Time series of tower base fore-aft BM, $V = 18$ m/s at hub height, normal wind shear, Coefficients set C.

4.2. Parametric correlation

A parametric correlation was performed to investigate the relationships between the most important parameters and the structural responses are presented in Fig. 16.

The hub-height wind speed (V), wind shear exponent (α), shutdown time (t_s), and three controller coefficients (k_P, k_I, and k_D) are regarded as the key influential parameters on the responses of the flapwise bending moment of blade 1 (*RtMy1*) and the main shaft bending moment (*BMSft*). As presented in the red shaded boxes, the wind speed, wind shear and the time instant when shutdown is triggered affect the blade root flapwise and main shaft bending moments experienced. Further, the blade root flapwise bending moments are strongly correlated to the main shaft bending

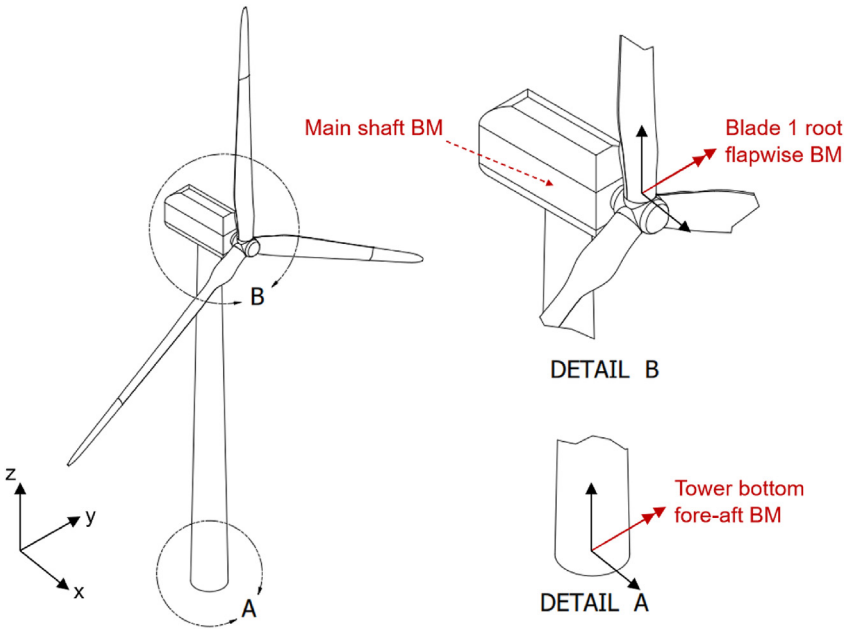

Fig. 21. Schematic of critical structural components of a land-based wind turbine.

moments (yellow shaded boxes). It is expected that the proportional coefficient k_P has a strong influence on the bending moment (purple shaded box). Moreover, it should be worthy of note that the derivative coefficient, k_D is an important control coefficient (green shaded box).

5. Results and discussion

5.1. Time series of selected response variables

For the selected wind conditions, representative time series of the blade root flapwise bending moment, the main shaft equivalent bending moment and the tower bottom fore-aft bending moment are presented. In the following, the OL method refers to the baseline open-loop emergency shutdown with a constant pitch rate of 8 deg/s. The FCS method has a variable pitch rate adjusted using the blade root flapwise bending moment errors.

5.1.1. Influence of the blade azimuth upon shutdown

We first carry out two simulations under the extreme wind shear condition. In these simulations, the shutdown times are adjusted so that blade 1 is either pointing upwards (azimuth = 0 deg) or pointing downwards (azimuth = 180 deg) upon shutdown. As shown in Fig. 17A and Fig. 18A, the shutdown times of these two illustrative examples differ from those specified in Table 1. This is because the load cases in Table 1 aims to cover different blade azimuth and it is convenient to initiate shutdown based on a specified shutdown time, T_s, rather than a specified blade azimuth in the aeroelastic code, FAST. When blade 1 has 0-deg azimuth, it has the largest wind loads among the three blades because of the wind shear, and the FCS method would initially make blade 1 pitch faster than the other two blades. When blade 1 has 180-deg azimuth, the wind loads on blade 2 are higher and the initial pitch rate of this blade is higher (Fig. 18A). Using the FCS method, the pitch rates of the three blades vary during the shutdown process. Because the FCS method aims to balance the bending moments of the blades, the individual flapwise bending moments of the blades might experience increased maximum loads during shutdown. For example, when blade 1 has a higher initial pitch rate, it experiences a reduction in the peak flapwise bending moment using the FCS method (Fig. 17C). The observation may be opposite when blade 1 has lower initial pitch rate; see Fig. 18C.

5.1.2. Extreme wind shear

Fig. 19A-C compare the effect of the OL method and the FCS method (coefficients set C) on the structural responses during emergency shutdown under the extreme wind shear and the rated wind condition. Among the structural responses, the flapwise bending moments of blades might experience increases during shutdown. This is less important, as the emergency shutdown does not cause higher extreme loads of blades than the operation phase. Interestingly, for the main shaft equivalent bending moment, the OL method with a collective blade pitch rate gives quite high extreme responses because of the aerodynamic load imbalance in the rotor plane. Compared to the OL method, the FCS method can reduce the extreme shaft bending moment by approximately 19% and reduce the following response fluctuations during shutdown (Fig. 19B). Similar observations can be found for the tower bottom fore-aft bending moment which also experiences large transient responses during shutdown; see Fig. 19C. The tower bottom bending moment reduces by about 14% (70971 kNm vs 60989 kNm) when the FCS is used. For the below- and above-rated wind conditions investigated, there are different magnitudes of structural responses during shutdown, but the effect of the FCS method is generally valid. Note that the effect of the FCS method varies depending on the PID coefficients used. This aspect will be discussed later in Section 5.4.

5.1.3. Normal wind shear

The structural responses under the normal wind shear and the above-rated wind condition are presented in Fig. 20A-C. Compared with the extreme wind shear and for a given wind speed and shutdown scenario, the normal wind shear results in less rotor imbalance, but the trend of the structural responses during shutdown are similar. After initiation of an emergency shutdown, both the flapwise bending moment and the tower bottom bending moment will first drop to a negative value and then oscillate around a small value close to zero, depending on wind conditions, and the

Table 4
Influence on maximum structural responses, extreme wind shear, coefficients set A (Most optimal).

V (m/s)	t_s (s)	Azimuth (deg)	Maximum structural responses								
			Blade 1 flapwise BM (kNm)			Main shaft BM (kNm)			Tower bottom fore-aft BM (kNm)		
			OL	FCS	%	OL	FCS	%	OL	FCS	%
8	70	46	6549	7534	15.0	4545	3342	-26.5	41365	38810	-6.2
	71	104	5648	4908	-13.1	4917	3819	-22.3	41776	40747	-2.5
	72	163	4736	3192	-32.6	4651	3455	-25.7	41500	36642	-11.7
	73	221	4736	3998	-15.6	4854	3950	-18.6	41581	37132	-10.7
	74	273	5816	5602	-3.7	4709	3603	-23.5	41729	38646	-7.4
	75	316	7312	7114	-2.7	4754	4065	-14.5	41232	39296	-4.7
11.4	70	39	11118	11510	3.5	6298	5219	-17.1	70972	68846	-3.0
	71	115	6462	6824	5.6	5689	4436	-22.0	72694	67237	-7.5
	72	194	6900	6309	-8.6	6000	5080	-15.3	73558	66072	-10.2
	73	272	8783	8803	0.2	5814	5251	-9.7	73280	69016	-5.8
	74	341	11419	11508	0.8	5739	4750	-17.2	74008	66488	-10.2
	75	36	9843	9816	-0.3	6260	5984	-19.3	73772	69530	-5.8
18	70	111	9150	9412	2.9	5753	5344	-7.1	77752	74791	-3.8
	71	186	4433	3538	-20.2	5270	5036	-4.5	77354	64163	-17.1
	72	259	4828	5413	12.1	6106	4954	-18.9	76600	62293	-18.7
	73	319	8078	8922	10.4	5769	5217	-9.6	78129	64470	-17.5
	74	7	10501	10457	-0.4	5936	5107	-14.0	77143	73512	-4.7
	75	43	9013	8011	-11.1	5779	5147	-10.9	77791	67703	-13.0

OL = Baseline (open loop) method; FCS = Feedback-controlled shutdown; % = percentage change, negative (marked in black) means a reduction in load, positive (marked in blue) means an increase.

main shaft equivalent bending moment will experience a peak response shortly after the blades are pitched to feather. Using the FCS method, both the peak main shaft bending moment and the tower bottom bending moment are effectively reduced by approximately 20% (Fig. 20B-C). Additionally, the FCS method also results in lower fluctuations in bending moments experienced at the blade, main shaft, and tower bottom. This leads to significantly lower short-term fatigue damage which will be presented in Section 5.3. For the below-rated and rated wind speeds, the influence of the FCS method on the structural responses is also investigated and the load reduction effects are on the same level as those for the above-rated wind speeds.

5.2. Influence on the extreme structural responses

The blade root flapwise bending moment, main shaft bending moment and tower bottom fore-aft bending moment can be regarded as critical structural responses for a land-based wind turbine [14]. A sketch is provided in Fig. 21 of the structural components and their positions in a wind turbine.

The influence of the FCS method on these structural responses is presented in Table 4 and Table 5 for the extreme wind shear and normal wind shear cases, respectively. The results are presented as a percentage difference according to Eq. (5.1),

$$\%diff = \frac{X_{PM} - X_{base}}{X_{base}} \times 100\% \tag{5.1}$$

where $\%diff$ is the percentage difference, X_{PM} is the response variable when the FCS method is applied and X_{base} is the response variable for the OL case.

The most optimal control coefficients (Coefficients set A) are used in these cases. Three main observations are made. First, there are several cases where the maximum blade 1 root flapwise bending moments may not be reduced. As previously discussed, this is because the focus of the controller is to balance the loads on the main shaft and loads on one or more blades could be increased. Second, the maximum tower bottom fore-aft bending moments reduce correspondingly with the maximum main shaft bending moments. Third, the effect of the load reduction is sensitive to the

Table 5
Influence on maximum structural responses, normal wind shear, coefficients set A (Most optimal).

V (m/s)	t_s (s)	Azimuth (deg)	Maximum structural responses								
			Blade 1 flapwise BM (kNm)			Main shaft BM (kNm)			Tower bottom fore-aft BM (kNm)		
			OL	FCS	%	OL	FCS	%	OL	FCS	%
8	70	46	5226	5182	-0.8	3324	2825	-15.0	40018	37940	-5.2
	71	104	5630	6417	14.0	3463	3073	-11.3	40003	43923	9.8
	72	163	6258	7809	24.8	3308	3037	-8.2	39699	37512	-5.5
	73	221	5636	5507	-2.3	3531	3094	-12.4	40223	38738	-3.7
	74	273	4398	4533	3.1	3270	2989	-8.6	39699	38913	-2.0
	75	316	4882	5030	3.0	3588	3040	-15.3	39955	43483	8.8
11.4	70	39	9718	11322	16.5	3936	3143	-20.1	69743	66320	-4.9
	71	115	9686	9976	3.0	4418	3504	-20.7	70032	66217	-5.4
	72	194	8777	8881	1.2	4045	3122	-22.8	69572	66372	-4.6
	73	272	8526	8954	5.0	4070	3431	-15.7	70004	66431	-5.1
	74	341	9147	9413	2.9	4458	3301	-26.0	69547	66455	-4.4
	75	36	9718	11428	17.6	3940	3425	-21.9	69722	66213	-5.0
18	70	111	7651	5571	-27.2	5101	3898	-23.6	80636	62603	-22.4
	71	186	5985	4789	-20.0	4745	3226	-32.0	80248	60899	-24.1
	72	259	5144	3694	-28.2	5310	3443	-35.2	80926	62347	-23.0
	73	319	6562	6343	-3.3	4582	3609	-21.2	80621	75583	-6.2
	74	7	7953	8308	4.5	4831	3534	-26.8	80346	63761	-20.6
	75	43	7591	6783	-10.6	5266	3692	-29.9	80947	67112	-17.1

OL = Baseline (open loop) method; FCS = Feedback-controlled shutdown; % = percentage change, negative (marked in black) means a reduction in load, positive (marked in blue) means an increase.

Table 6
List of the S–N curve parameters[a].

Component	Material	log($\bar{a}$)	m	E (Gpa)
Blade	GRP	−11.776	7.651	12
Main shaft	Steel	15.117	4.0	210
Tower	Steel	15.117	4.0	210

m: negative inverse slope of S–N curve.
E: Young's modulus.
[a] **log($\bar{a}$)**: Intercept of mean S–N curve with the log N axis.

Table 7
Geometric data of interested structural components.

Component	Location	Geometry	Diameter (m)	Thickness (m)
Blade	Root	Hollow circle	1.5	0.20
Main shaft	Along the shaft	Solid circle	2.0	–
Tower	Bottom	Hollow circle	6.0	0.027

shutdown time. This is expected because different shutdown times are associated with different blade azimuth and instantaneous loading conditions. For the extreme wind shear (Table 4), the reduction percentage of the main shaft moment generally is more than 10%. For the normal wind shear (Table 5) the reduction percentage of the main shaft moment generally is greater than 20%.

5.3. Influence on the short-term fatigue damage

In this section, the short-term fatigue damages of the blade root flapwise bending, main shaft bending moment, and tower bottom fore-aft bending moment during the emergency shutdowns are investigated. Although shutdowns occur less frequently than operational conditions, a considerable number of shutdowns can occur during the lifetime of a wind turbine.

The short-term fatigue damage is calculated using Miner's rule [29] as presented in Eq. (5.2).

Table 8
Influence on short term fatigue damage, extreme wind shear, Coefficients A (Most optimal).

V (m/s)	t_s (s)	Azimuth (deg)	Short term fatigue damage[1]		
			Blade 1 flapwise BM	Main shaft BM	Tower bottom fore-aft BM
8	70	46	75.9	-61.3	-4.2
	71	104	-47.5	-85.4	-2.3
	72	163	-47.8	-81.0	-59.7
	73	221	32.4	-69.8	-57.7
	74	273	-0.7	-72.3	-10.4
	75	316	29.9	-75.5	-13.6
11.4	70	39	-47.7	-81.0	-31.9
	71	115	-32.7	-89.5	-51.0
	72	194	-2.9	-88.5	-28.1
	73	272	1.4	-46.8	-21.2
	74	341	32.5	-66.1	-28.7
	75	36	-1.6	-55.7	-22.6
18	70	111	1.9	-15.1	-29.5
	71	186	-88.4	-20.4	-64.6
	72	259	169.6	-83.8	-69.4
	73	319	83.5	-46.8	-57.7
	74	7	6.4	-68.1	-3.2
	75	43	-77.3	-61.1	-41.6

[1] Negative (marked in black) means a reduction in short term fatigue damage; positive (marked in blue) means an increase in the fatigue damage.

$$D = \sum_i \frac{n_i}{N_i} \tag{5.2}$$

where D is the accumulated short-term fatigue damage, n_i is the number of cycles experienced for stress range $\Delta\sigma_i$ and N_i is the allowable number of cycles for stress range $\Delta\sigma_i$. N_i can be calculated using the SN curve equation as presented in Eq. (5.3) and Eq. (5.4) for the main shaft and tower (steel material) and blade (composite material), respectively.

$$\log N_i = \log\bar{a} - m \log(\Delta\sigma_i) \tag{5.3}$$

$$\log N_i = \log\bar{a} - m \log\left(\frac{\Delta\sigma_i}{2E}\right) \tag{5.4}$$

where $\log\bar{a}$ and m are the S–N curve parameter constants and E is the Young's modulus. Eq. (5.3) is a strain-cycle S–N curve which is the normal way S–N curves for composite materials are presented. This contrasts with the stress-cycle S–N curve for steel materials. The S–N curve parameters used are presented in Table 6.

The composite S–N curve data is obtained from Ref. [3] while the steel S–N curve data is the B1 curve (in air) from Ref. [30]. The geometric data at the locations of the components where fatigue damages are calculated are presented in Table 7.

We focus on the extreme wind shear condition as this condition may lead to excessive fatigue damage. The short-term fatigue damages are calculated for 20 s after a shutdown initiation. The

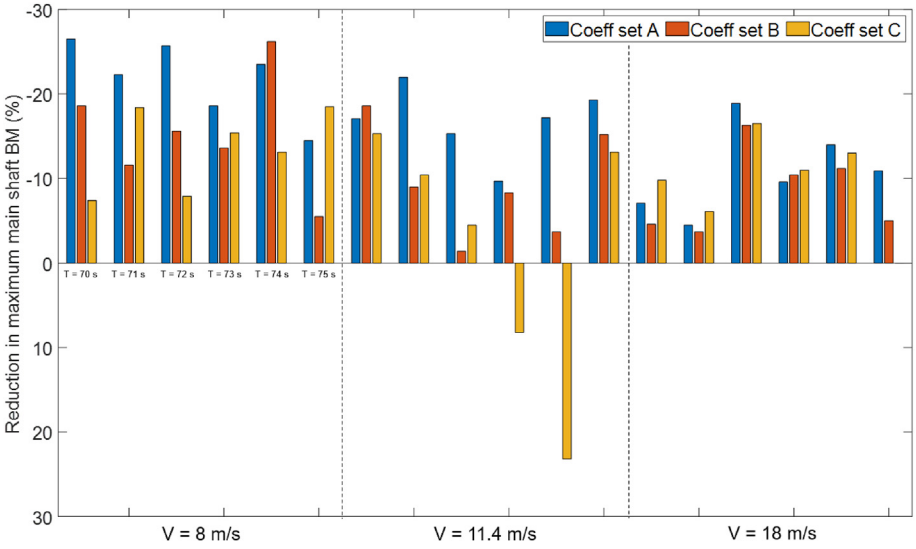

Fig. 22. Reduction[1] in main shaft BM versus control coefficients, extreme wind shear, [1]Negative means load reduction.

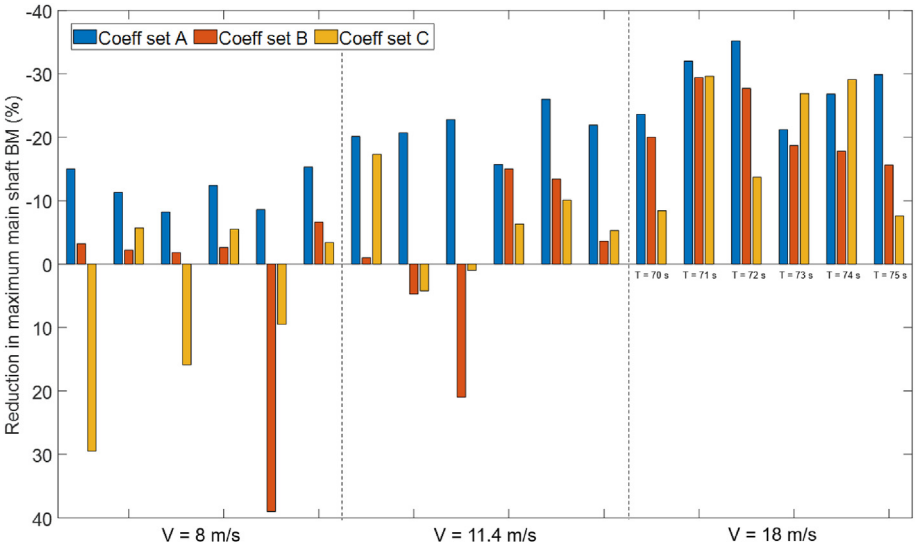

Fig. 23. Reduction[1] in main shaft BM versus control coefficients, normal wind shear, [1]Negative means load reduction.

results are presented in Table 8 as percentage difference according to Eq. (5.1). Control coefficients set A, i.e., the most optimal coefficients are used.

In general, the short-term fatigue damages are significantly reduced for the main shaft and the tower bottom. The average reduction in the main shaft bending moment is more than 60% under the extreme wind shear. The reduction in the tower bottom bending moment is less than that in the main shaft bending moment but can still exceed 30% under the extreme wind shear. This highlights the effectiveness of the FCS method in reducing loads and consequently short-term fatigue damages when appropriate control coefficients are used. There are cases where the short-term fatigue damages can increase for Blade 1. As mentioned, this is because in the process of trying to balance the loads on the main shaft, loads on one or more blades could be increased.

5.4. Discussion of the controller performance

The FCS method will always reduce the main shaft bending moment if appropriate controller gains of Coefficient set A are applied. The results presented in Fig. 22 and Fig. 23 show that there are reductions in the main shaft bending moment experienced for each load case considered. The reductions for many load cases are more than 20%. This means that a reduction in the main shaft bending moment can be always achieved if the appropriate controller gains are applied. This demonstrates the functionality of the FCS method. Further, optimised control coefficients also lead to the largest bending moment reduction (Coefficient set A). Optimised control coefficient for individual load cases can be implemented using a gain-scheduling control algorithm.

The FCS method generally works well when averaged coefficients (Coefficients sets B and C) are used. There are only a few cases where the FCS method performs sub-optimally when averaged coefficients were utilised; the number of cases with deteriorated performance are larger for the normal wind shear case. Using the averaged coefficients of Coefficients sets B and C generally leads to a decrease in performance, i.e., less reduction or even increase in the main shaft bending moment. The above highlights the ability of the method, though simple, to reduce loads during most shutdown events.

Although the FCS method works well for most of the load cases considered in this paper, the controller can be significantly improved by adopting model predictive control (MPC) methods. Using MPC methods such as the ones presented in Ref. [31]; the controller will have the ability to anticipate the future load effects and take appropriate control actions to minimise the main shaft bending moments. In practice, this would mean that the controller would have ability to optimise the controller gains at every time step based on load predictions performed slightly ahead in time.

6. Concluding remarks

In this work, we propose a simple load mitigation method for reducing the structural responses of wind turbines during emergency shutdown. Unlike the conventional open-loop strategy for pitch-to-feather shutdowns, the proposed shutdown method uses a feedback control and considers the blade root flapwise bending moments as an important indicator of the rotor imbalance. The control algorithm is implemented in the simulation platform FAST-SIMULINK and aeroelastic simulations are performed under several wind conditions. The main conclusions are as follows:

- The feedback-controlled shutdown can effectively reduce the extreme nontorque bending moment on the shaft and the tower bottom fore-aft bending moment during emergency shutdowns. Under the extreme and normal wind shear conditions investigated, the reduction in these structural responses can vary between 10% and 40% using the optimal PID coefficients. However, the blade bending moment will not necessarily decrease.
- The feedback-controlled shutdown also effectively reduces the large cycle oscillations and hence the short-term fatigue damage of several structural responses. Under the extreme wind shear condition investigated, the reduction in the shaft and the tower bottom fatigue damage can generally reach 60% using the optimal PID coefficients.
- The performance of the proposed controller is sensitive to the blade azimuth upon shutdown and the controller coefficients used. For practical applications under complex environmental conditions, active gain scheduling or model predictive control is needed to optimise the load mitigation effects.

Although the present analysis is limited to a land-based wind turbine, future work can include extending the application to floating offshore wind turbines.

CRediT authorship contribution statement

Zhiyu Jiang: Methodology, Writing – original draft, Writing – review & editing. **Yihan Xing:** Methodology, Writing – original draft, Writing – review & editing.

Declaration of competing interest

The authors declare that they have no known competing financial interests or personal relationships that could have appeared to influence the work reported in this paper.

References

[1] P.S. Veers, S. Butterfield, Extreme load estimation for wind turbines: issues and opportunities for improved practice, in: AIAA Aerospace Science Meeting, 2001.
[2] K. Ronold, G. Larsen, Reliability-based design of wind-turbine rotor blades against failure in ultimate loading, Eng. Struct. 22 (6) (2000) 565–574.
[3] K.O. Ronold, J. Wedel-Heinen, C.J. Christensen, Reliability-based fatigue design of wind-turbine rotor blades, Eng. Struct. 21 (12) (1999) 1101–1114.
[4] Z. Jiang, Y. Xing, Y. Guo, T. Moan, Z. Gao, Long-term contact fatigue analysis of a planetary bearing in a land-based wind turbine drivetrain, Wind Energy 18 (4) (2014) 591–611.
[5] T.J. Larsen, H.A. Madsen, K. Thomsen, Active load reduction using individual pitch, based on local blade flow measurements, Wind Energy 8 (1) (2005) 67–80.
[6] H. Namik, K. Stol, Individual blade pitch control of floating offshore wind turbines, Wind Energy 13 (1) (2009) 74–85.
[7] Z. Zhang, J. Li, S.R. Nielsen, B. Basu, Mitigation of edgewise vibrations in wind turbine blades by means of roller dampers, J. Sound Vib. 333 (21) (2014) 5283–5298.
[8] Z. Zhang, A. Staino, B. Basu, S.R. Nielsen, Performance evaluation of full-scale tuned liquid dampers (TLDs) for vibration control of large wind turbines using real-time hybrid testing, Eng. Struct. 126 (2016) 417–431.
[9] Germanischer Lloyd Industrial Services GmbH, Guideline for the Certification of Wind Turbines, 2010. Hamburg, Germany.
[10] A. Munoz, E.F. Sánchez-Ubeda, A. Cruz, J. Marín, Short-term forecasting in power systems: a guided tour, in: Handbook of Power Systems II, Springer, 2010, pp. 129–160.
[11] Z. Jiang, M. Karimirad, T. Moan, Dynamic response analysis of wind turbines under blade pitch system fault, grid loss, and shutdown events, Wind Energy 17 (9) (2013) 1385–1409.
[12] S. Anlas, ENERCON E-82 Technical Description, 2005.
[13] IEC, in: International Electrotechnical Commission, IEC 61400–1 Wind Turbine Part 1: Design Requirements, third ed., IEC, Geneva, Switzerland, 2007.
[14] Z. Jiang, T. Moan, Z. Gao, A comparative study of shutdown procedures on the dynamic responses of wind turbines, J. Offshore Mech. Arctic Eng. 137 (1) (2015), 011904.
[15] A.R. Nejad, Z. Jiang, Z. Gao, T. Moan, Drivetrain load effects in a 5-MW bottom-fixed wind turbine under blade-pitch fault condition and emergency shutdown, in: Journal of Physics: Conference Series, IOP Publishing, 2016.
[16] P. Louazel, D. Son, B. Yu, Impact of a wind turbine blade pitch rate on a floating wind turbine during an emergency shutdown operation, in: ASME 2020 39th International Conference on Ocean, Offshore and Arctic Engineering, American Society of Mechanical Engineers Digital Collection, 2020.
[17] C. Luan, T. Moan, On short-term fatigue analysis for wind turbine tower of two semi-submersible wind turbines including effect of startup and shutdown processes, J. Offshore Mech. Arctic Eng. 143 (1) (2021), 012003.
[18] E. Fırtın, Ö. Güler, S.A. Akdağ, Investigation of wind shear coefficients and their effect on electrical energy generation, Appl. Energy 88 (11) (2011) 4097–4105.
[19] Minnesota Department of Commerce, Wind Resource Analysis Program (WRAP), Minnesota Department of Commerce, St. Paul, Minnesota, USA, 2002.
[20] E. Otto, M. Durstewitz, B. Lange, The RAVE research initiative: a successful collaborative research, development and demonstration programme, in: Ecological Research at the Offshore Windfarm Alpha Ventus, Springer Spektrum, Wiesbaden, 2014, pp. 25–29.
[21] J. Jonkman, FAST User's Guide, National Renewable Energy Lab. (NREL), Golden, CO (United States), 2009.
[22] L. Frøyd, O.G. Dahlahug, Effect of pitch and safety system design on dimensioning loads for offshore wind turbines during grid fault, Energy Proc. 24 (2012) 36–43.
[23] M.H. Hansen, Aeroelastic instability problems for wind turbines, Wind Energy 10 (6) (2007) 551–577.
[24] J.K. Lee, J.Y. Park, K.Y. Oh, S.H. Ju, J.S. Lee, Transformation algorithm of wind turbine blade moment signals for blade condition monitoring, Renew. Energy 79 (2015) 209–218.
[25] J. Jonkman, S. Butterfield, W. Musial, G. Scott, Definition of a 5-MW Reference Wind Turbine for Offshore System Development (No. NREL/TP-500-38060), National Renewable Energy Lab. (NREL), Golden, CO (United States), 2009.
[26] J. Jonkman, W. Musial, Offshore Code Comparison Collaboration (OC3) for IEA Wind Task 23 Offshore Wind Technology and Deployment (No. NREL/TP-5000-48191), National Renewable Energy Lab.(NREL), Golden, CO (United States), 2010.
[27] W. Popko, F. Vorpahl, A. Zuga, M. Kohlmeier, J. Jonkman, A. Robertson, T.J. Larsen, A. Yde, K. Sætertrø, K.M. Okstad, J. Nichols, June. Offshore Code Comparison Collaboration Continuation (OC4), Phase 1-Results of Coupled Simulations of an Offshore Wind Turbine with Jacket Support Structure. The Twenty-Second International Offshore and Polar Engineering Conference, 2012.
[28] S. Wang, T. Moan, Z. Jiang, Influence of variability and uncertainty of wind and waves on fatigue damage of a floating wind turbine drivetrain, Renew. Energy 181 (2021) 870–897.
[29] M.A. Miner, Cumulative damage in fatigue, J. Appl. Mech. 12 (3) (1945) A159–A164.
[30] DNV, Recommended Practice: Fatigue Design of Offshore Steel Structures (DNV-RP-C203), 2011. Høvik, Norway.
[31] L.C. Henriksen, Model Predictive Control of Wind Turbines, , PhD thesis,, Technical University of Denmark, 2011.